Dalton Transactions

PAPER

Cite this: *Dalton Trans.*, 2017, **46**, 12516

Cadmium–1,4-cyclohexanedicarboxylato coordination polymers bearing different di-alkyl-2,2′-bipyridines: syntheses, crystal structures and photoluminescence studies†

Luis D. Rosales-Vázquez,[a] Víctor Sánchez-Mendieta,[a,b]* Alejandro Dorazco-González,*[b] Diego Martínez-Otero,[b] Iván García-Orozco,[a] Raúl A. Morales-Luckie,[b] Jonathan Jaramillo-Garcia[a] and Antonio Téllez-López[a]

Four coordination polymers have been synthesized using self-assembly solution reactions under ambient conditions, reacting Cd(II) ions with 1,4-cyclohexanedicarboxylic acid in the presence of different 2,2′-bipyridine co-ligands: $\{[Cd(H_2O)(e,a\text{-}cis\text{-}1,4\text{-chdc})(2,2'\text{-bpy})]\cdot H_2O\}_n$ (**1**); $[Cd_2(H_2O)_2(e,a\text{-}cis\text{-}1,4\text{-chdc})_2(4,4'\text{-dmb})_2]_n$ (**2**); $\{[Cd(e,a\text{-}cis\text{-}1,4\text{-chdc})(5,5'\text{-dmb})]\cdot H_2O\cdot CH_3OH\}_n$ (**3**) and $\{[Cd(e,e\text{-}trans\text{-}1,4\text{-chdc})(4,4'\text{-dtbb})]\cdot CH_3OH\}_n$ (**4**), where 1,4-chdc = 1,4-cyclohexanedicarboxylato, 2,2′-bpy = 2,2′-bipyridine, 4,4′-dmb = 4,4′-dimethyl-2,2′-bipyridine, 5,5′-dmb = 5,5′-dimethyl-2,2′-bipyridine and 4,4′-dtbb = 4,4′-di-*tert*-butyl-2,2′-bipyridine. Crystallographic studies show that compound **1** has a 1D structure propagating along the crystallographic *b*-axis; the Cd ion in **1** is six-coordinated with a distorted-octahedral coordination sphere. Compound **2** has two crystallographic different Cd ions and both are six-coordinated with a distorted-octahedral coordination sphere. Compound **3** exhibits a seven-coordinated Cd ion having a distinctive distorted-monocapped trigonal prismatic geometry. In compound **4**, the Cd ion is also seven-coordinated in a distorted monocapped octahedral geometry. Compounds **2**, **3** and **4** possess rhombic-shaped dinuclear units (Cd_2O_2) as nodes to generate larger cycles made up of four dinuclear units, a Cd_4 motif, bridged by four 1,4-chdc ligands, accomplishing, thus, 2D structures. Remarkably, in compound **4** the 1,4-chdc ligand conformation changes to the *equatorial*, *equatorial trans*, unlike the other compounds where the bridging ligand conformation is the more typical *equatorial*, *axial cis*. The solid state luminescence properties of **1–4** were investigated; polymers **3** and **4** exhibited a strong blue emission (λ_{em} = 410–414 nm) compared to **1** and **2**; structure-related photoluminescence is attributed to the degree of hydration of the compounds. Furthermore, Cd-polymer **3** suspended in acetone allows the fluorescence selective sensing of acetonitrile over common organic solvents such as alcohols and DMF, based on turn-on fluorescence intensity with a limit of 53 μmol L^{-1}.

Received 1st July 2017,
Accepted 26th August 2017

DOI: 10.1039/c7dt02376f

rsc.li/dalton

Introduction

Investigation about the fundamental properties of coordination polymers has gained relevance due mainly to the synergic relationship between structural and physicochemical properties. Particularly, the search for tailor-made synthetic methodologies capable of producing desired properties for applications of these types of hybrid materials has long been pursued.[1–3] The design and synthesis of coordination polymers based on the assembly of metal ions and bridging-multidentate organic ligands has resulted in one of the fastest growing areas in synthetic chemistry, which has been powered by the captivating structural diversity and potential applications of these hybrid materials in gas absorption, magnetism, drug delivery, separation processing, catalysis and chemical sensing.[4–8] Several strategies have been developed to synthesize mixed ligand coordination polymers of transition metals containing nitrogen and oxygen donor ligands.[9–12] Self-assembly of small molecules, compounds or complexes is demonstrated to be an effective procedure for the synthesis of

[a]*Facultad de Química, Universidad Autónoma del Estado de México, Paseo Colón y Paseo Tollocan, Toluca, Estado de México 50120, Mexico. E-mail: vsanchezm@uaemex.mx*

[b]*Centro Conjunto de Investigación en Química Sustentable UAEM-UNAM, Carretera Toluca-Ixtlahuaca Km. 14.5, Tlachaloya, Toluca, Estado de México, Mexico. E-mail: adg@unam.mx*

†Electronic supplementary information (ESI) available: FTIR spectra, TGA, fluorescence spectra, bond lengths and bond angle tables for **1** to **4**. CCDC 1555262, 1555263, 1555264 and 1555265 for **1** to **4**, respectively. For ESI and crystallographic data in CIF or other electronic format see DOI: 10.1039/c7dt02376f

extended structures with minimum effort. Nonetheless, the self-assembly process is sometimes accompanied by an uncertainty halo, due to unpredictable interactions among metal centers and ligands, especially when weak forces (*e.g.*, hydrogen bonding, π–π interactions) and/or solvents, such as water, are involved.[13] Something encouraging in this simple methodology is the usual formation of supramolecular structures, generated by the presence of unreacted ends of ligands and/or the presence of water molecules both as aqua ligands and crystallization molecules. These supramolecular extended structures bring novel and interesting structural characteristics to the coordination polymers, which also, in some cases, influence their properties. Among the most used bridging ligands for transition metal ions are the dicarboxylato ligands.[14–17] The 1,4-cyclohexanedicarboxylato ligand has been used for the formation of coordination polymers with different metal centers.[17–20] We have selected this metal center-bridging ligand due to its interesting chemical structure and its dual chemical functionality, which allows generation of complexes or polymers with different dimensionalities depending on its coordination modes. Moreover, the use of 2,2′-bipyridine as an ancillary ligand had become relevant in our previous studies on coordination polymers.[21,22] Therefore, as part of our ongoing research about complexes and coordination polymers of dicarboxylates and 2,2′-bipyridines several of these compounds with interesting structural, magnetic and luminescence properties have been achieved through self-assembly reactions under ambient conditions.[23–25] Thus, we decided to use one of the most studied nitrogen donor ligands,[26] and just varying the alkyl-substituent on it to verify the possible influence of the steric hindrance and the π–π interactions of this co-ligand on the dimensionality and crystalline structures of cadmium coordination polymers. To date, there have been only a few reports on the use and study of di-alkyl-2,2′-bipyridines as ancillary ligands, either in transition-metal complexes[27] or in coordination polymers.[28] It is well known that photoluminescence properties of coordination polymers can be controlled by the appropriate choice of organic ligands and metal centers. These properties are usually dependent on the metal center nature and its coordination environment, or coordination sphere, the presence of conjugation in the organic ligand and the nature of substituents on the ligands in addition to the possible supramolecular interactions in the extended structure.[29–33] Many of the luminescent materials studied are lanthanide and d^{10} metal based coordination polymers with multidentate aromatic bridging ligands;[34–36] however, there are less of these luminescent materials containing non-aromatic linkers,[35] such as the 1,4-cyclohexanedicarboxylato ligand. Most of these compounds have been referenced in the literature for their capacity of sensing of hazardous substances.[36–40]

Herein, the syntheses, structural characterization, thermogravimetric and photoluminescence studies of four new coordination polymers constructed by self-assembly: {[Cd(H_2O)(*e*,*a-cis*-1,4-chdc)(2,2′-bpy)]·H_2O}$_n$ (**1**); [$Cd_2(H_2O)_2$(*e*,*a-cis*-1,4-chdc)$_2$(4,4′-dmb)$_2$]$_n$ (**2**); {[Cd(*e*,*a-cis*-1,4-chdc)(5,5′-dmb)]·H_2O·CH_3OH}$_n$ (**3**) and {[Cd(*e*,*e-trans*-1,4-chdc)(4,4′-dtbb)]·CH_3OH}$_n$ (**4**), are presented and discussed.

Experimental section

Materials and general methods

All the materials of reagent grade were purchased from commercial sources and used without further purification. Deionized water was used for synthetic procedures. Elemental analyses for C, H, and N were carried out by standard methods using a Vario Micro-Cube analyzer. IR spectra of the complexes were recorded on a FT-IR Shimadzu spectrophotometer, IR Prestige-21, from 4000–400 cm^{-1}. Thermogravimetric analyses were performed using a TA Instruments equipment, under a N_2 atmosphere, at a heating rate of 10 °C min^{-1}, from 20 to 800 °C.

Synthesis of {[Cd(H_2O)(*e*,*a-cis*-1,4-chdc)(2,2′-bpy)]·H_2O}$_n$ (1)

Firstly, sodium 1,4-cyclohexanedicarboxylate was prepared by adding NaOH (5 ml; 0.16 M) to a methanol solution (5 ml) of 1,4-cyclohexanedicarboxylic acid (0.0688 g; 0.4 mmol). A solution of 2,2′-bipyridine (0.0624 g; 0.4 mmol) in methanol (5 ml) was added to the solution of sodium 1,4-cyclohexanedicarboxylate while stirring. Then, a de-ionized water solution (10 ml) of $Cd(NO_3)_2$·$4H_2O$ (0.0624 g; 0.4 mmol) was added. A colorless translucent solution was obtained. After two days, big white crystals were obtained; these were filtered out and washed with a 50 : 50 deionized water–methanol mixture. Yield: 79% based on the metal precursor. Elemental analysis (%), $C_{18}H_{22}N_2O_6Cd$, cal.: C, 45.53; H, 4.67, N, 5.90; found: C, 45.40; H, 4.70; N, 5.92. IR cm^{-1} (ATR): 3277 (w, br), 2951 (w, br), 1573 (m, br), 1531 (m, br), 1442 (m, br), 1392 (s, br), 763 (s, sh), 732 (m, sh), 678 (m, sh).

Synthesis of [$Cd_2(H_2O)_2$(*e*,*a-cis*-1,4-chdc)$_2$(4,4′-dmb)$_2$]$_n$ (2)

Comparable conditions as in the synthesis of **1** were employed, except that a solution of 4,4-dimethyl-2,2′-bipyridine (0.0720 g; 0.4 mmol) in methanol (10 ml) was added to the solution of sodium 1,4-cyclohexanedicarboxylate while stirring. Then, a solution of $Cd(NO_3)_2$·$4H_2O$ (0.0624 g; 0.4 mmol) in de-ionized water (10 ml) was added. A colorless translucent solution was obtained. After four days, big white crystals were obtained; these were filtered out and washed with a 50 : 50 deionized water–methanol mixture. Yield: 41% based on the metal precursor. Elemental analysis (%), $C_{40}H_{48}N_4O_{10}Cd_2$, cal.: C, 49.54; H, 4.98; N, 5.77; found: C, 49.19; H, 5.03; N, 5.76. IR cm^{-1} (ATR): 3034 (w, br), 2943 (w, br), 1612 (w, sh), 1566 (s, sh), 1442 (m, sh), 1384 (s, sh), 833 (s, sh), 771 (m, sh), 717 (m, sh).

Synthesis of {[Cd(*e*,*a-cis*-1,4-chdc)(5,5′-dmb)]·H_2O·CH_3OH}$_n$ (3)

Similar conditions as in the synthesis of **1** were used, except that a solution of 5,5′-dimethyl-2,2′-bipyridine (0.0720 g; 0.4 mmol) in methanol (10 ml) was added to the solution of sodium 1,4-cyclohexanedicarboxylate. A colorless translucent solution was obtained. After five days, big white crystals were

obtained; these were filtered out and washed with a 50 : 50 deionized water–methanol mixture. Yield: 72% based on the metal precursor. Elemental analysis (%), $C_{21}H_{28}N_2O_6Cd$, cal.: C, 48.79; H, 5.45, N, 5.42; found: C, 48.61; H, 5.42; N, 5.53. IR cm^{-1} (ATR): 3402 (w, br), 2927 (w, sh), 1562 (s, sh), 1543 (s, sh), 1481 (m, sh), 1400 (s, sh), 1045 (s, sh), 844 (m, sh), 732 (m, sh), 762 (w, sh).

Synthesis of {[Cd(*e*,*e-trans*-1,4-chdc)(4,4′-dtbb)]·CH_3OH}$_n$ (4)

Analogous conditions as in the synthesis of **1** were used, except that a solution of 4,4′-di-*tert*-butyl-2,2′-bipyridine (0.1073 g; 0.4 mmol) in methanol (10 ml) was added to the solution of sodium 1,4-cyclohexanedicarboxylate. A colorless translucent solution was obtained. After a few days, big white crystals were obtained; these were filtered out and washed with a 50 : 50 deionized water–methanol mixture. Yield: 94% based on the metal precursor. Elemental analysis (%), $C_{27}H_{38}N_2O_5Cd$, cal.: C, 55.63; H, 6.57, N, 4.80; found: C, 56.20; H, 5.98; N, 6.13. IR cm^{-1} (ATR): 3086 (w, br), 2954 (w, sh), 1608 (m, br), 1546 (s, br), 1454 (m, br), 1395 (s, sh), 848 (m, sh), 678 (s, sh), 601 (s, sh).

Photoluminescence measurements

Luminescence spectra for solid state and suspensions of polymers **1–4** were recorded on an Agilent Cary Eclipse spectrophotometer equipped with a crystal holder or a cell thermostated holder with a quartz cuvette. In all cases, single crystalline samples of **1–4** were used for emission measurements. Suspensions of **1–4** were prepared by stirring for 20 min at 25 °C of the corresponding crystal samples of polymers **1–4** in spectrophotometric grade solvents (acetone, acetonitrile, *n*-butanol, dichloromethane, tetrachloromethane, *n*-butanol, ethanol, ethyl acetate, methanol isopropanol, and tetrahydrofuran) and water with a concentration of 2.0 mg mL^{-1}. For titration experiment of acetonitrile, a stock suspension of **3** (1.0 mg mL^{-1}) in acetone was prepared by ultrasonic treatment by 10 min at r.t. and subsequently, 40 μL of this suspension was diluted up on 2500 μL of water, to give a final concentration of 30 μM and the emission spectra of the suspension were recorded after adding aliquots of acetonitrile.

X-ray crystallography

Data for compounds **1** to **4** were collected on a Bruker APEX II CCD diffractometer; **2** and **3** at 100 K, and **1** and **4** at room temperature (296 K); using Mo-Kα radiation (k = 0.71073 Å) from an Incoatec ImuS source and a Helios optic monochromator.[41] Suitable crystals were coated with hydrocarbon oil, picked up with a nylon loop, and mounted in the cold nitrogen stream of the diffractometer. The structures were solved using intrinsic phasing (SHELXT)[42] and refined by full-matrix least-squares on F^2 (ref. 42) using the ShelXle GUI.[43] The hydrogen atoms of the C–H bonds were placed in idealized positions whereas the hydrogen atoms from the O–H moieties and hydrogens for water were localized from the difference electron density map and fixed to standard distances using DFIX instructions, and their position was refined with U_{iso} tied to the parent atom with distance restraints. Owing to the data collection temperature polymers **1** and **4** exhibit positional disorder, **1** shows positional disorder in cyclohexane-1,4-dicarboxylate and water molecule and the molecule with which it forms a hydrogen bridge interaction, the majority part has an occupancy of 63.5(4)%, forming two types of nets for hydrogen interactions one in each part of the disorder. Also, **4** exhibits positional disorder in the *tert*-butyl moieties of the bipyridine ligand; the part 1 in the first *tert*-butyl moiety (C11, C12, C13, and C14) has an occupancy of 61.2(12)%, the part 1 in the second majority *tert*-butyl moiety (C15, C16, C17, and C18) has an occupancy of 72.3(18)%, and the solvent also has positional disorder; the majority part has an occupancy of 71.5(5)% and only part 1 in the solvent has a hydrogen bond toward the oxygen (O2) in the carboxylate moiety. Compounds **2** and **3** have a good crystal packing and have no positional disorder, due to the data collection temperature. The disorder in **1** and **4** was refined using geometry (SADI, SAME) and U_{ij} restraints (SIMU, RIGU) implemented in SHELXL,[42] the occupancy is refined with the help of a free variable and fixed at unit.

Details of crystal data and refinement parameters, bond lengths and angles are provided in Tables S1–S4† for **1–4**, respectively.

Results and discussion

Crystal and molecular structure of {[Cd(H_2O)(*e*,*a-cis*-1,4-chdc)(2,2′-bpy)]·H_2O}$_n$ (1)

1 crystallizes in a monoclinic system with the $P2_1/c$ space group and forms an infinite one-dimensional (1D) coordination polymer (Fig. 1). The repeat molecular unit contains one Cd center, one 1,4-chdc ligand, one 2,2′-bpy co-ligand, one coordinated water and one guest H_2O molecule. The coordination environment of the Cd is shown in Fig. 1A; the metal is six-coordinated and surrounded by four oxygen atoms, three from two different 1,4-chdc ligands and one from the aqua ligand, plus two nitrogen atoms from one 2,2′-bpy ligand. The Cd has a distorted octahedral configuration. The Cd–O bond lengths range from 2.289(5) to 2.473(13) Å, while the Cd–N distances are 2.3439(19) and 2.378(2) Å and these values are comparable to those found for similar Cd(II) compounds.[44,45] In polymer **1**, a 1D zig-zag chain is formed due to the combination of monodentate η^1 and chelating η^2 coordination modes in 1,4-chdc, together with the *equatorial*, *axial cis* conformation of its carboxylate groups, thus bridging the Cd ions (Fig. 1B and Scheme S1†). In fact, a cadmium 2D coordination polymer having 1,4-cyclohexanedicarboxylate and 2,2′-bipyridine has been reported.[46] However, it was obtained by a solvothermal method, and its molecular, polymeric and supramolecular structural characteristics, and thus its crystallographic properties, are different from the ones obtained for **1**. Intermolecular hydrogen-bonding interactions assemble polymer **1** into a 2D supramolecular array. These interactions are promoted by the presence of the aqua ligand.[47] This is shown in Fig. 1C, where the main O–H···O interactions involve

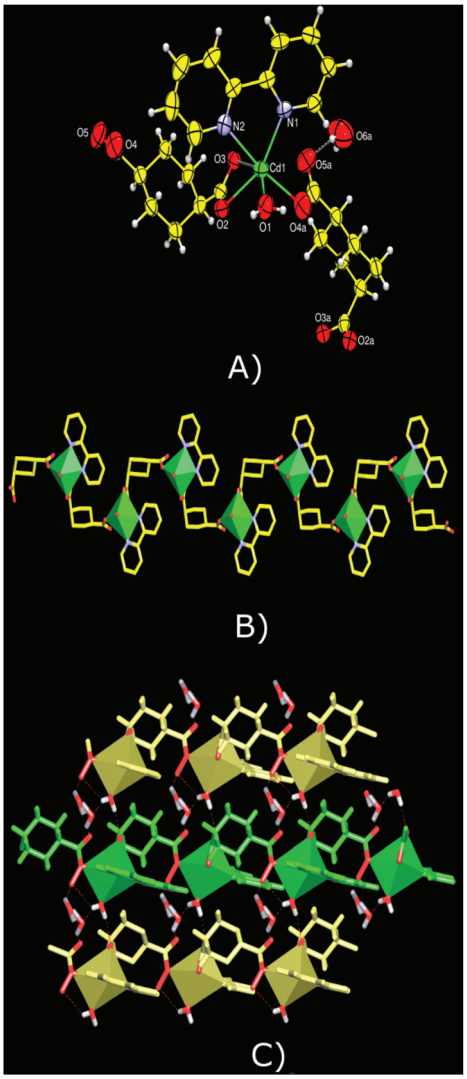

Fig. 1 (A) Molecular structure; (B) 1D polymer chain, hydrogen atoms are omitted for clarity; (C) 2D supramolecular array, most hydrogen atoms are omitted for clarity; in **1**.

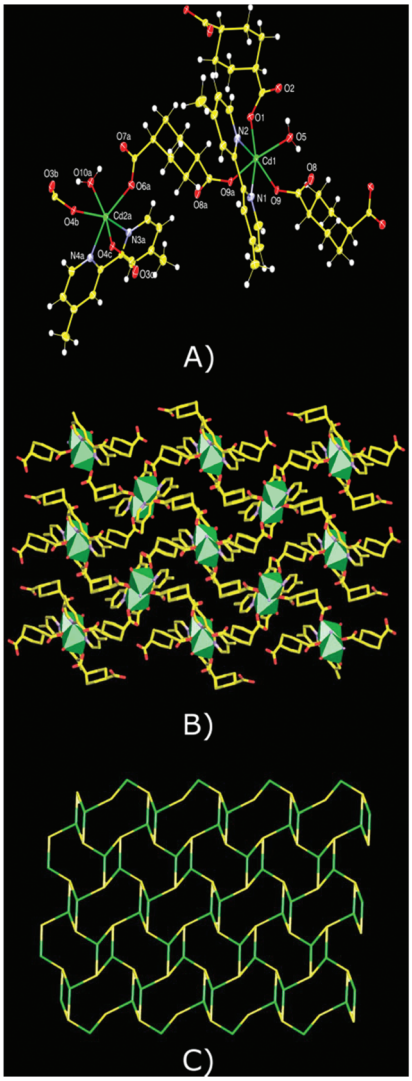

Fig. 2 (A) Molecular structure; (B) 2D polymer array, hydrogen atoms are omitted for clarity; (C) simplified topological network; in **2**.

the O–H moiety (O1) of the aqua ligand and each oxygen atom (O3) of the coordinated side of one 1,4-chdc ligand of a neighboring 1D polymeric chain, in an intermolecular hydrogen bond (Table S1†). Thus, an extended 2D supramolecular array in a corrugated sheet shape is generated (Fig. 1C).

Crystal and molecular structure of $[Cd_2(H_2O)_2(e,a\text{-}cis\text{-}1,4\text{-}chdc)_2(4,4'\text{-}dmb)_2]_n$ (2)

2 crystallizes in a triclinic system with the $P\bar{1}$ space group and forms an infinite two-dimensional (2D) coordination polymer. The molecular structure of **2** consists of two crystallographically independent Cd^{2+} centers, two 1,4-chdc ligands, two 4,4′-dmb ligands and two aqua ligands (Fig. 2A). Both Cd atoms are six-coordinated, being surrounded by four oxygen atoms from two different 1,4-chdc ligands plus the oxygen atom from the aqua ligand, and two nitrogen atoms from one 4,4′-dmb co-ligand, in a distorted octahedral configuration. The Cd–O bond lengths vary from 2.2028(14) to 2.3557(14) Å, while the Cd–N distances range from 2.2931(16) to 2.4088(16) Å, values comparable to those found in the related Cd(II) complexes.[48,49] The dimensionality of this Cd coordination polymer can be explained by the occurrence of two different coordination modes of the carboxylate moieties of the 1,4-chdc ligand: η^1 and bridging μ_2–η^2; the latter generating distinctive rhombic-shape dinuclear units (Cd_2O_2). These two different coordination modes of the 1,4-chdc ligand give rise to a 2D sheet array (Fig. 2B and Scheme S1†). Following the carboxylate-bridge coordination modes, this dimeric unit in **2** possesses a *syn–syn* configuration and an *equatorial–equatorial* conformation arrangement. In a broader view, another 1,4-chdc ligand binds to these Cd centers in a bridging mono-dentate manner, as mentioned above, connecting the rhomboid Cd dimers to larger fusion-cycles made of four Cd ions all linked and bridged by four 1,4-chdc ligands in an *equatorial–axial cis* conformation of their carboxylate groups (Fig. 2B). Hence, the

2D structure of **2** can be classified as a uninodal 5-connected net with the *tts* topology and the point symbol of $\{3^3{\cdot}4^3{\cdot}5^4\}$ (Fig. 2C).[50] The crystal packing of **2** is stabilized also by hydrogen bonds. Adjacent complex units are connected by hydrogen bonds between the carboxylato oxygen atoms of 1,4-chdc: O(5)–H(5B)···O(2); O(5)–H(5A)···O(8); O(10)–H(10A)···O(3) and O(10)–H(10B)···O(7) (Table S2†). Nevertheless, these interactions do not change the structural dimensionality of **2**.

Crystal and molecular structure of {[Cd(*e*,*a*-*cis*-1,4-chdc)(5,5′-dmb)]·H_2O·CH_3OH}$_n$ (3)

3 crystallizes in a monoclinic system with the $P2_1/c$ space group and forms an infinite two-dimensional (2D) coordination polymer. The repeat molecular unit of **3** consists of one Cd center, two 1,4-chdc ligands, one 5,5′-dmb ligand, one guest methanol molecule and one crystallization water molecule (Fig. 3A). Thus, the Cd ion is seven-coordinated, being surrounded by five oxygen atoms from two different 1,4-chdc ligands and two nitrogen atoms from one 5,5′-dmb co-ligand, resulting in a N_2O_5, still rare, distorted-monocapped trigonal prismatic geometry.[51] The capping oxygen atom (O2) comes from one of the carboxylate oxygen atoms in 1,4-chdc (Fig. 3A). The obtuse angles between the least-squares mean planes of the chelate ring of 5,5′-dmb, the chelate rings of the pairs of the oxygens O1 and O3 and O1 and O4 of 1,4-chdc, and the metal, lie in the range 91.69–147.06°, which is in concordance with a distorted trigonal prismatic coordination geometry. For **3**, the lengths of the triangular sides are in the range of 2.740–3.621 Å for the triangle O1–N2–O1 and 2.195–3.357 Å for the triangle O3–N1–O4, all angles are in the range 38.34–75.95°. Four 1,4-chdc oxygen atoms (two O1, O3, O4) make up a trapezoid, which should be a perfect square for an ideal trigonal-prismatic geometry, the sides of which are in the range of 2.740–3.254 Å. The remaining two faces of the prism are also trapezoids consisting of four oxygen atoms of the 1,4-chdc ligand, which are joined by the two nitrogen atoms of the 5,5′-dmb ligand, respectively. Both faces have a O–O distance of 3.230 and 3.254 Å, an N–O distance in the range of 3.125–3.621 Å, and 2.698 Å for the N1–N2 side. Due to these marked differences in the distances of the trapezoid faces of the prism, the two triangular faces are not parallel. Thus, the planes defined by O3–N2–O4 and O1–N2–O1 make an angle of 18.93°. The torsion angles about the centroids of the triangular faces and each of the corners (*i.e.*, Ct1–N1–N2–Ct2) are 19.71, 16.10 and 3.58°. To the best of our knowledge, there are few examples reported in the literature about metaprism complexes with innocent ligands in their structures,[52] and, also few articles showing Cd(II) coordination polymers having a distorted-monocapped trigonal prismatic geometry without the use of tri- or tetradentate ligands.[53]

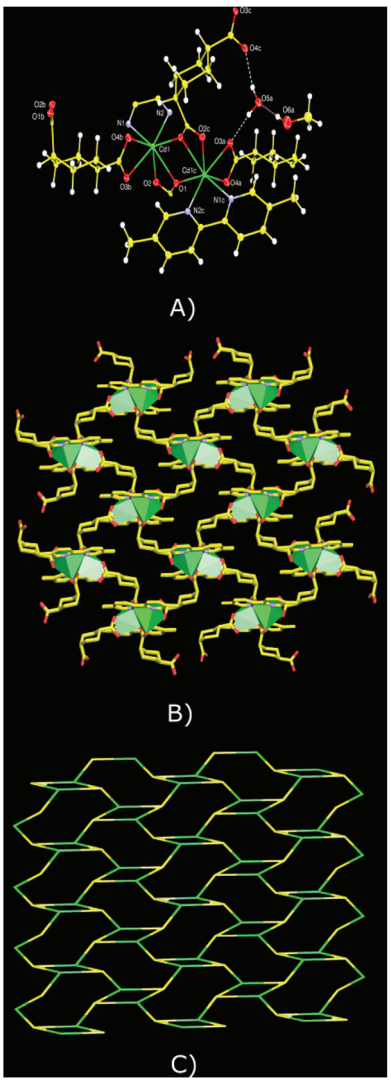

Fig. 3 (A) Molecular structure, (B) 2D polymer array, hydrogen atoms are omitted for clarity; (C) simplified topological network; in **3**.

Therefore, complexes or coordination polymers of Cd using mixed innocent bidentate ligands possessing trigonal prismatic, or monocapped trigonal prismatic, are still considered uncommon. Like in polymer **2**, the dimensionality of **3** can be elucidated by the existence of two different coordination modes of the carboxylate moieties of the 1,4-chdc ligand: chelating μ_2–η^2 and chelating, bridging μ_2–η^2:η^1; this latter mode generates the distinctive rhombic-shape dinuclear units (Cd_2O_2) (Scheme S2†). Thus, compound **3** also displays the dinuclear units as nodes to generate larger cycles made up of four dinuclear units, a Cd_4 motif, bridged by four 1,4-chdc ligands, accomplishing a 2D structure with a *tts* topological framework[50] (Fig. 3B and C), similar to compound **2**. The crystal structure of **3** is stabilized also by hydrogen bonds: O(5)–H(5B)···O(4) and O(5)–H(5A)···O(3), which are formed by the presence of a crystallization water molecule (Table S3†). These interactions do not alter the structural dimensionality of **3**.

Crystal and molecular structure of {[Cd(*e*,*e*-*trans*-1,4-chdc)(4,4′-dtbb)]·CH_3OH}$_n$ (4)

4 crystallizes in a triclinic system with the $P\bar{1}$ space group and forms an infinite two-dimensional (2D) coordination polymer.

The repeat molecular unit of **4** consists of one Cd center, two 1,4-chdc ligands, one 4,4′-dtbb ligand and one guest methanol molecule (Fig. 4A). Thus, the Cd ion is seven-coordinated, being surrounded by five oxygen atoms from two different 1,4-chdc ligands and two nitrogen atoms from one 4,4′-dtbb co-ligand, resulting in a N_2O_5, distorted monocapped octahedral geometry. The capping atom comes from one of the carboxylate oxygen atoms (O1) in the chelating, bridging (μ_2–η^2:η^1) coordination mode of 1,4-chdc in polymer **4** (Fig. 4A). The alternation of two different coordination modes in the bridging 1,4-chdc ligand of **4** is rather unusual; there is one with chelating μ_2–η^2 mode in both carboxylate ends, and then, comes another ligand with bridging μ_2–η^2:η^1, also at both ends (Fig. 4A and Scheme S2†). Remarkably, in both types of alternating coordination modes, the 1,4-chdc ligand in **4** appears in an *equatorial*, *equatorial-trans* conformation; although this conformation is thermodynamically more stable, it is not always found in this ligand when forming coordination polymers.[54] As in polymers **2** and **3**, the bridging μ_2–η^2:η^1 coordination mode generates the distinctive rhombic-shape dinuclear units (Cd_2O_2). Thus, compound **4** also displays the dinuclear units as nodes to generate larger cycles made up of four dinuclear units, a Cd_4 motif, bridged by four 1,4-chdc ligands, accomplishing also a 2D structure with a uninodal 6-connected layer, exhibiting a new topology, according to TOPOS[50] software analysis, with the point symbol of $\{3^6{\cdot}4^6{\cdot}5^3\}$ (Fig. 4B and C). In the structure of **4** there is only one hydrogen bond: O(5)–H(5)···O(3), which is formed by the presence of the crystallization methanol molecule (Table S4†). This interaction does not modify the structural dimensionality of **4**.

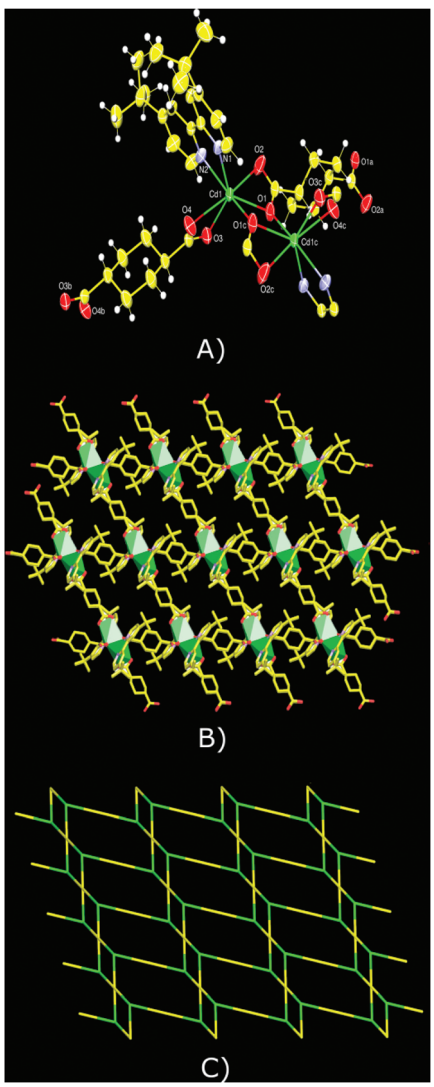

Fig. 4 (A) Molecular structure; (B) 2D polymer array, hydrogen atoms are omitted for clarity; (C) simplified topological network; in **4**.

Without doubt, the diverse coordination modes of dicarboxylates, and of the 1,4-chdc ligand with the Cd ion, as in polymers **1** to **4** (Scheme 1), promote the generation of rather fascinating coordination arrays. Interestingly, the most recurring coordination mode of the 1,4-chdc ligand in these compounds is the bridging μ_2–η^2:η^1, followed by the chelating μ_2–η^2 mode. The non-appearance of the bridging μ_2–η^2:η^1 mode seems to be the main chemical characteristic responsible for yielding a 1D polymer in **1**, instead of a 2D extended structure as obtained in the other polymers. Moreover, it appears that in polymer **2** the chelating coordination mode in 1,4-chdc is restricted due to a certain steric hindrance produced by the alkyl-substituents in the auxiliary ligand; however, the intramolecular hydrogen bridging, promoted by the presence of an aqua ligand and the uncoordinated oxygen atom: O(5)–H(5B)···O(2); O(5)–H(5A)···O(8); O(10)–H(10A)···O(3) and O(10)–H(10B)···O(7), seems to be the most influential structural feature to preclude the appearance of the chelating coordination mode of the 1,4-chdc ligand in **2**. Consequently, in polymers **2** and **4** the coordination modes of the 1,4-chdc ligand appear to allow further space for better accommodation of the 4,4′-dmb and 4,4′-dtbb auxiliary ligands, respectively. Even more, the through-space distance between two metal centers, across the 1,4-chdc bridge, in polymer **1** is 8.357 Å and in polymer **3** it is 8.667 Å, which, as expected, are very close values; meanwhile, the same type of distance among metal centers in compounds **2** and **4** is 9.052 and 11.457 Å, respectively. The latter value is considerably longer because of the rare *equatorial*, *equatorial*, *equatorial-trans* conformation adopted by the 1,4-chdc ligand in **4**. The fact that polymer **1** is the only compound that exhibits a supramolecular structure, demonstrates also that the less hindered structure of the 2,2′-bpy auxiliary ligand in **1** allows further connections to stabilize its structure in the solid state.

IR and TGA analyses

The IR spectra of the four complexes show the typical bands expected for carboxylate ligands coordinated to Cd(II),[55] along with the bands corresponding to the auxiliary ligands (Fig. S1–S4†). The main variances may come from the different coordination modes acquired by the 1,4-chdc bridging ligands in these complexes. The IR spectrum of complex **1** shows two sets of asymmetric stretches for the carboxylate moiety at 1570 and

1527 cm^{-1}, with the corresponding symmetric stretches at 1392 and 1491 cm^{-1}. The differences between asymmetric and symmetric stretches for the carboxylate ion ($\Delta\nu_{COO^-}$) are 178 and 96 cm^{-1}, respectively. These bands can be assigned to the bidentate chelate and monodentate coordination modes of the 1,4-chdc ligand in **1**. In **2**, there are also two sets of asymmetric stretches for the carboxylate moiety at 1564 and 1555 cm^{-1}, with the corresponding symmetric stretches at 1385 and 1443 cm^{-1}. The separations of the two sets of bands are as expected for the bridging (179 cm^{-1}) and the monodentate (112 cm^{-1}) coordination forms, respectively. In **3**, the asymmetric carboxylate stretch occurs at 1562 cm^{-1} along with the symmetric stretch at 1400 cm^{-1}, the separation of the two bands (162 cm^{-1}) is as expected primarily for the chelating coordination form. Similarly, in **4**, the asymmetric carboxylate stretch occurs at 1551 cm^{-1} along with the symmetric stretch at 1396 cm^{-1}, the separation of the two bands (155 cm^{-1}) corresponds mainly to a chelating coordination mode.[56]

To examine the thermal stabilities of the crystalline polymers, thermal analyses were performed for complexes **1–4** between 20 and 700 °C (Fig. S5†). The polymers show a stepwise loss of weight, exhibiting three main stages of decomposition. The first weight loss occurs between 90 and 180 °C; the second, with a weight loss of ~45% of the initial weight, takes place approximately between 218 and 418 °C. The final weight loss (~20%) occurs around 312–510 °C, after which only 1.21–5.34% of the initial sample weight remains. In all complexes, the first decomposition stage can be ascribed to the loss of crystallization water or methanol; however, for complex **1**, crystallization water and coordinated water are lost, while for complex **2**, only coordinated water is lost. In **3**, crystallization water and one crystallization methanol are lost; and, in **4**, only one crystallization methanol is lost. The higher temperature stages can be attributed to the combined weight loss of the 1,4-chdc ligand, followed by the corresponding bipyridine co-ligands. Curiously, polymer **1** seems to be the most thermally robust of the complexes, while polymer **4** is the least.

Photoluminescence studies

In the solid-state, **3** and **4** exhibit a similar blue photoluminescence emission under ambient conditions with bands centred at 409 and 414 nm upon excitation at 330 and 345 nm, respectively, as is shown in Fig. 5. In contrast, crystals of **1** practically do not exhibit emission and **2** presents a modest emission at 389 nm (λ_{ex} = 330 nm) but with lower intensity than those observed for **3** and **4**. The emission broad bands centred at 389–414 nm for **2–4** can be attributed to effective interaction of the di-alkyl-bpy ligands (4,4′-dmb, 5,5′-dmb, 4,4′-dtbb) to the Cd(II) ion with a bathochromic shift by comparison to the very weak fluorescence emission of the free alkylated bpy ligands at ambient temperature.[57] It is well-known that the enhancement of the fluorescence intensity of bpy-based ligands on complexation with d^{10} transition metals, is due to the increase of the rigidity of the aromatic ligand in the final supramolecular arrangement which reduces the loss of energy through non-radiative processes.[57–60] Similar photochemical properties with emission bands in the range of 380–450 nm have been reported previously for several Zn(II)/Cd(II) coordination polymers containing aromatic [N,N]-chelating ligands as 2,2′-bpy derivatives and multi-carboxylate anions as linkers; for recent examples see: $[Cd_{1.5}(dpob)(2,2'\text{-bpy})]$,[61] $[Cd_2(phthalate)(2,2'\text{-bpy})_2]$,[62] $[Zn(dcbpy)(DMF)]$[63] and $[Cd(tptc)_{0.5}(2,2'\text{-bipy})]$[64] (dpob = 3-(2′,3′-dicarboxylphenoxy)-benzoic acid; dcbpy = 2,2′-bipyridine-4,4′-dicarboxylate and L = (1,1′:4′,1″-terphenyl)-2′,3,3″,5′-tetracarboxylic acid), where the position of the emission peak is related to the involvement of the auxiliary 2,2′-bpy ligand.[62,65] The emission maxima in this range wavelengths is usually assigned to a ligand-to-metal charge transfer process (LMCT)[57,66] in combination with a strongly perturbed π–π* and π–n* transition, namely, ligand-to-ligand charge transfer (LLCT).[59,67,68] The considerable blue fluorescence intensity of **3** and **4** compared to a modest emission of **2** or null fluorescence of **1**, can be a result of the absence of coordinated water molecules in **3** and **4**, which are efficient quenchers.[69] In order to explore the potential chemosensing properties of **3** and **4**, their photoluminescence spectra of liquid suspensions in several pure organic solvents and water, with constant stirring, were analyzed. Fig. 6 shows the family of the spectra (λ_{exc} = 340 nm) of **3** (1.0 mg mL^{-1}), a similar spectral behaviour was observed for **4** (Fig. S6†). Among the studied solvents, CH_3CN showed the highest intensity (λ_{em} = 412 nm), followed by chlorinated solvents (CCl_4, λ_{em} = 416 nm; CH_2Cl_2, λ_{em} = 412 nm) but their emission is significantly lower than that observed for acetonitrile. All alcohols (CH_3OH, EtOH, i-PrOH and *n*-ButOH) and THF exhibited a modest emission with limited change in their maxima (λ_{em} = 402–412 nm). Suspensions in acetone and water do not present emission. Taking this into account, we used acetone as suspension medium for carrying out a solvent sensing experiment, owing to its miscibility with all solvents used and its ability to turn-on fluorescence by addition of non-polar solvents such as CH_3CN or chlorinated solvents.

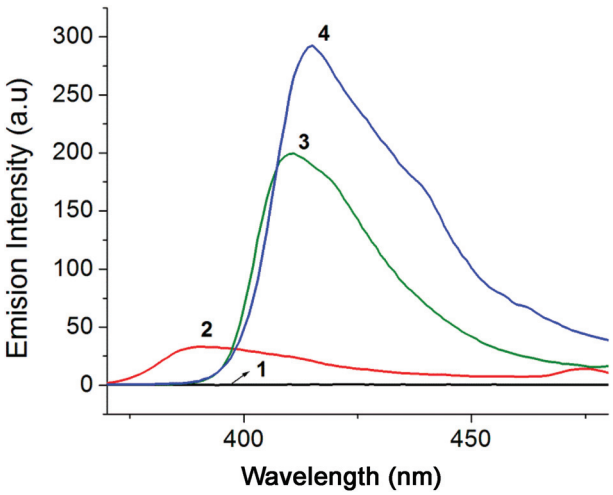

Fig. 5 Solid-state emission spectra of **1–4** at room temperature. **2** and **3** (λ_{exc} = 330 nm) and **4** (λ_{exc} = 345 nm).

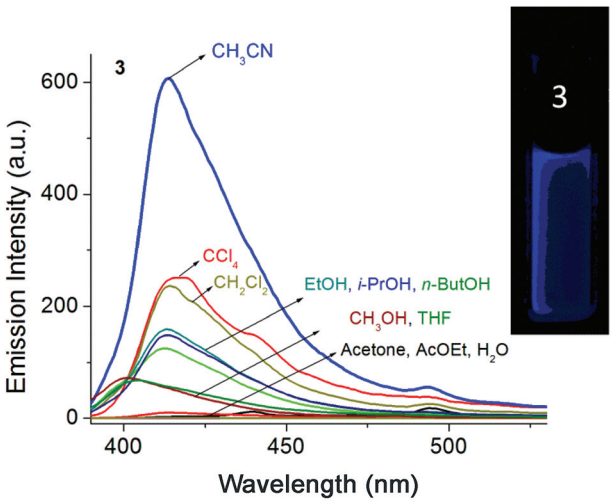

Fig. 6 Emission spectra of **3** (λ_{exc} = 340 nm) at room temperature in different pure organic solvents and water. The inset shows acetonitrile suspension of 3 under irradiation at 365 nm UV-light.

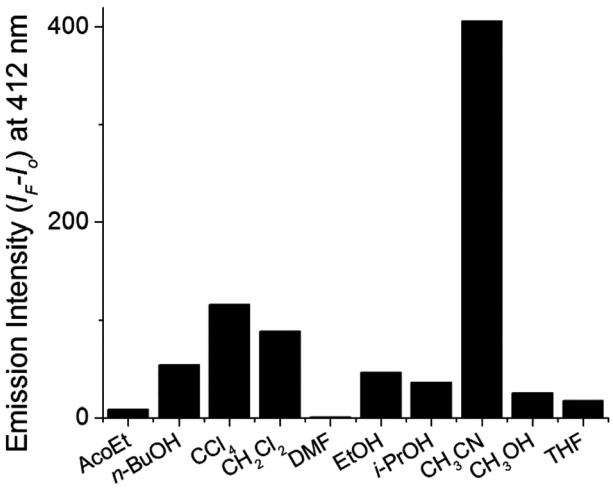

Fig. 7 Fluorescence intensity changes at 412 nm (λ_{exc} = 340 nm) of acetone suspension of **3** upon addition of 30.0 equiv. of different organic solvents.

Due to the chemical, environmental and industrial importance of volatile organic solvents, there is a constant and growing interest in the development of new optical sensors where the mechanism relies on an increase of fluorescence intensity, rather than quenching, because this limits seriously their practical applications. Currently, the vast majority of coordination polymers used for sensing of organic solvents induce fluorescence quenching and they are active for alcohols, aromatic solvents, acetone and DMF,[66,70] interestingly, the literature features only a few examples for acetonitrile sensing.[71,72] In this line, two flexible and interpenetrated networks of Cd(II)–organic frameworks containing biphenyldicarboxylic acid have been reported as sensitive fluorescent sensors for CH_3CN involving an exchange of the crystallization water molecules by acetonitrile.[73] Thus, the solvent selectivity of an acetone suspension of **3** (≈30 μM) was examined by addition of 30.0 equiv. of different organic solvents and the emission intensity increase at 412 nm was recorded. All alcohols, AcOEt, DMF and THF gave a very low response (Fig. 7). Interestingly, **3** displays sensitive sensing with respect to acetonitrile. The addition of dichloromethane and tetrachloromethane provokes a modest turn-on fluorescence signal of ≈29% of that observed for acetonitrile. A careful comparison of the emission spectra (Fig. 6) reveals a similar blue shift in response to all alcohols and THF molecules in comparison with CH_3CN; on the other hand, chlorinated solvents exhibit a similar maxima emission around 412 nm. Based on this fact, the enhancement of photoluminescence and selectivity for acetonitrile could be presumably attributed to the distinctive effects of non-polar solvent molecules on the luminescent units (5,5′-dmb), particularly for a dehydration process, which can be attributed to an efficient dynamic exchange of water molecules, initially encapsulated in the host assembly of **3**, by acetonitrile. A PLATON program analysis shows that there is about 33% of the crystal volume accessible to solvents.[74] This exchange phenomena involving organic small-molecule solvents has been largely studied even in interpenetrated coordination polymers.[72,73]

In order to probe the utility of **3** as a sensor, a fluorescence titration experiment was carried out by addition of increasing amounts of acetonitrile to a suspension of **3** (≈30 μM) in acetone under the same conditions as those used in the experiment shown in Fig. 7. Since the emission intensity of the acetonitrile suspension is the strongest of the used solvents the acetone suspension did not exhibit emission. The addition of CH_3CN (0–50 equiv.) induced a considerable turn-on fluorescence signal with maxima at 412 nm (Fig. 8). At elevated concentration of acetonitrile ($[CH_3CN]_{tot}$ = 1.5 mM, 50 equiv.), the photoluminescence spectrum resembled that recorded in

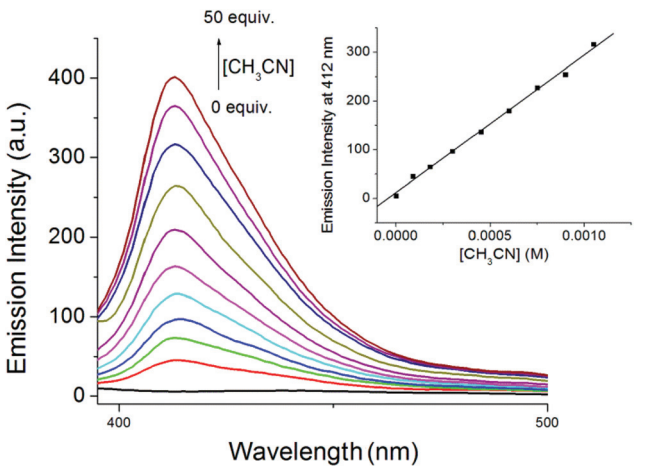

Fig. 8 Changes of the emission spectra (λ_{ex} = 340 nm) of acetone suspension of **3** upon addition of increasing amounts of CH_3CN (0–1.5 mM). The inset shows the calibration curve with a linear fit at λ_{em} = 412 nm.

the pure acetonitrile suspension (Fig. 6). For the concentration range of [CH_3CN] < 900 μM, the emission shows a linear dependence as shown in Fig. 8 (inset). The detection limit (LOD) for complex **3** with CH_3CN, defined as LOD = $3\sigma/s$, where σ is the standard deviation of the blank signals and s is the slope of the calibration curve with the linear fit (inset, Fig. 8), is 53 μM. Thermogravimetric analysis and FT-IR spectra of the as-synthesized **3**, and of a sample of this polymer treated with acetonitrile by stirring at room temperature, were performed and compared to investigate the dynamic solvent exchange and why the fluorescence was turned-on by addition of acetonitrile molecules (Fig. 9A). TGA of **3** revealed mass losses in the range of 65–94 °C, assigned to the release of crystallization methanol/water molecules, and no further mass loss is observed until 300 °C. On the other hand, treating polymer **3** with CH_3CN at room temperature results in the loss of its crystallinity and a different thermal behaviour with a loss of mass at a higher temperature of about 80–110 °C in comparison with that observed with the starting material, which can be ascribed to the presence of CH_3CN (Fig. 9B). The decomposition process of polymer-treated **3** was observed until 360 °C. Finally, the FTIR spectrum of a crystalline sample of **3** after its treatment with acetonitrile, filtered-off and dried under vacuum, shows characteristic bands (cm^{-1}) for this solvent at 2293 (CH_3 stretch), 2253 (CN stretch), 1376 (CH_3 s-deformation) (Fig. S7†) indicating that acetonitrile is able to replace, at least partially, methanol/water molecules in **3**. Recently, a Cd(II)-polymer has been reported as a sensor material for detection of nitroaromatic compounds, which exhibits a strong emission intensity in dispersed acetonitrile with reversible emission and recyclability properties based on solvent–analyte (nitrocompound) exhange.[75] Additionally, the enhancement of luminescence emission in coordination polymers induced by inclusion of non-polar small molecules as organic solvents, has been attributed to the fact that these molecules can affect the intramolecular ligand–metal energy transfer (LMET).[76]

In general, these results establish that the potential physical interactions between **3** and organic small-molecule solvents have a large effect on its fluorescence properties.

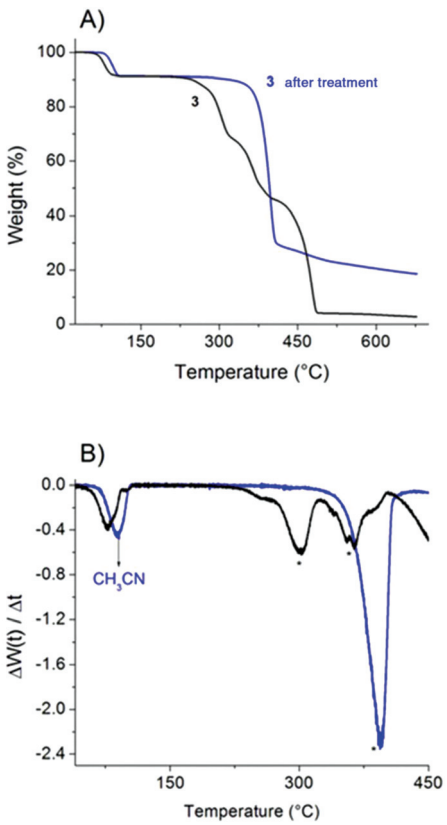

Fig. 9 (A) TGA of a crystalline sample of the as-synthesized polymer **3** (black), and after treated with CH_3CN (blue). (B) First-derivative TGA plots for solvent exchange, acetonitrile-modified polymer **3**. *Decomposition of polymer **3**.

Conclusions

In summary, four coordination polymers of Cd(II), $\{[Cd(H_2O)(e,a\text{-}cis\text{-}1,4\text{-}chdc)(2,2'\text{-}bpy)]\cdot H_2O\}_n$ (**1**); $[Cd_2(H_2O)_2(e,a\text{-}cis\text{-}1,4\text{-}chdc)_2(4,4'\text{-}dmb)_2]_n$ (**2**); $\{[Cd(e,a\text{-}cis\text{-}1,4\text{-}chdc)(5,5'\text{-}dmb)]\cdot H_2O\cdot CH_3OH\}_n$ (**3**) and $\{[Cd(e,e\text{-}trans\text{-}1,4\text{-}chdc)(4,4'\text{-}dtbb)]\cdot CH_3OH\}_n$ (**4**), were obtained by self-assembly *via* solution reactions under ambient conditions. X-ray crystallography studies revealed a 1D structure for **1**, with a 2D supramolecular array; whereas polymers **2–4** possess 2D structures, with *tts* topological frameworks for **2** and **3**, and for **4**, a novel topology with a uninodal 6-connected layer and a point symbol of $\{3^6\cdot4^6\cdot5^3\}$. Photoluminescence properties of **3** and **4**, in the solid-state and suspensions in acetonitrile, show that they possess blue emission with maxima at 410–414 nm. Cd(II)-Polymer **3**, suspended in acetone, can be used as a luminescent material for the detection of acetonitrile in the micromolar concentration range. Under these conditions, the addition of acetonitrile exhibits a rapid and selective response, based on turn-on fluorescence intensity, over common organic solvents such as alcohols and DMF; only chlorinated organic solvents elicit a significant interference. This outstanding sensing property of **3** toward CH_3CN and CCl_4, in combination with the high-yield simplified synthesis, makes it a promising candidate for the design of more sensitive materials with application in sensing of environmental-pollutant small molecules.

Conflicts of interest

There are no conflicts of interest to declare.

Acknowledgements

Authors are indebted to M. en C. Alejandra Nuñez Pineda and M. en C. Lizbeth Triana Cruz (CCIQS UAEM-UNAM) for elemental and FTIR analyses, respectively. Funding for this work was provided by Universidad Autónoma del Estado de

México (UAEM). We are thankful to CONACyT (CB239648 and PDCPN247495) and UNAM (PAPIIT-IN207317) for financial support.

References

1 R. Robson, *Dalton Trans.*, 2008, 5113.
2 B. F. Abrahams, S. R. Batten, H. Hamit, B. F. Hoskins and R. Robson, *Angew. Chem., Int. Ed. Engl.*, 1996, **35**, 1690.
3 M. Eddaoudi, J. Kim, N. Rosi, D. Vodak, J. Wachter, M. O'Keeffe and O. M. Yaghi, *Science*, 2002, **295**, 469.
4 L. Xue, F. Luo, Y. Che and J. Zheng, *J. Mol. Struct.*, 2007, **832**, 132.
5 K. T. Youm, M. G. Kim, J. Ko and M. J. Jun, *Angew. Chem., Int. Ed.*, 2006, **45**, 4003.
6 D. R. Talham and M. W. Meisel, *Chem. Soc. Rev.*, 2011, **40**, 3356.
7 C.-Y. Sun, C. Qin, X.-L. Wangand and Z.-M. Su, *Expert Opin. Drug Delivery*, 2013, **10**, 89.
8 S. Kitagawa, R. Kitaura and S.-I. Noro, *Angew. Chem., Int. Ed.*, 2004, **43**, 2334.
9 M. Dua, C.-P. Li, C.-S. Liub and S.-M. Fang, *Coord. Chem. Rev.*, 2013, **257**, 1282.
10 J.-P. Zhang, Y.-B. Zhang, J.-B. Lin and X.-M. Chen, *Chem. Rev.*, 2012, **112**, 1001.
11 F. A. A. Paz, J. Klinowski, S. M. F. Vilela, J. P. C. Tomé, J. A. S. Cavaleiro and J. Rocha, *Chem. Soc. Rev.*, 2012, **41**, 1088.
12 S.-H. Li, S.-K. Gao, S.-X. Liu and Y.-N. Guo, *Cryst. Growth Des.*, 2010, **10**, 495.
13 M. D. Allendorf and V. Stavila, *CrystEngComm*, 2015, **17**, 229.
14 D. Curiel, M. Más-Montoya and G. Sánchez, *Coord. Chem. Rev.*, 2014, **284**, 19.
15 S. J. Bora and B. K. Das, *J. Solid State Chem.*, 2012, **192**, 93.
16 T. A. Beard, J. A. Wilson and R. L. LaDuca, *Inorg. Chim. Acta*, 2017, **466**, 30.
17 T.-F. Liu, J. Lü and R. Cao, *CrystEngComm*, 2010, **12**, 660.
18 D. Sun, M.-Z. Xu, S.-S. Liu, S. Yuan, H.-F. Lu, S.-Y. Feng and D.-F. Sun, *Dalton Trans.*, 2013, **42**, 12324.
19 J. Chen, M. Ohba, D. Zhao, W. Kaneko and S. Kitagawa, *Cryst. Growth Des.*, 2006, **6**, 664.
20 I. H. Kim, X. Wang and A. J. Jacobson, *Solid State Sci.*, 2010, **12**, 76.
21 B. O. Patrick, W. M. Reiff, V. Sanchez, A. Storr and R. C. Thompson, *Polyhedron*, 2001, **20**, 1577.
22 B. O. Patrick, W. M. Reiff, V. Sanchez, A. Storr and R. C. Thompson, *Inorg. Chem.*, 2004, **43**, 2330.
23 A. Téllez-López, J. Jaramillo-García, R. Martínez-Domínguez, R. A. Morales-Luckie, M. A. Camacho-López, R. Escudero and V. Sánchez-Mendieta, *Polyhedron*, 2015, **100**, 373.
24 J. Jaramillo-García, A. Téllez-López, R. Martínez-Domínguez, R. A. Morales-Luckie, D. Martínez-Otero, V. Sánchez-Mendieta and R. Escudero, *J. Coord. Chem.*, 2016, **69**, 1525.
25 A. Téllez-López, V. Sánchez-Mendieta, J. Jaramillo-García, L. D. Rosales-Vázquez, I. García-Orozco, R. A. Morales-Luckie, R. Escudero and F. Morales-Leal, *Transition Met. Chem.*, 2016, **41**, 879.
26 R. D. Hancock, *Chem. Soc. Rev.*, 2013, **42**, 1500.
27 R. Alizadeh and V. Amani, *Inorg. Chim. Acta*, 2016, **443**, 151.
28 L. B. Lopes, C. C. Corrêa, G. P. Guedes, M. G. F. Vaz, R. Diniz and F. C. Machado, *Polyhedron*, 2013, **50**, 16; G. M. Zhang, Y. Li, X. Z. Zou, J. A. Zhang, J. Z. Gu and A. M. Kirillov, *Transition Met. Chem.*, 2016, **41**, 153.
29 Y. M. You and S. Y. Park, *Dalton Trans.*, 2009, 1267.
30 H.-X. Ju, *Front. Chem.*, 2013, **1**, 1.
31 X.-L. Wang, F.-F. Sui, H.-Y. Lin, J.-W. Zhang and G.-C. Liu, *Cryst. Growth Des.*, 2014, **14**, 3438.
32 L. Cui, G.-P. Yang, W.-P. Wu, H.-H. Miao, Q.-Z. Shi and Y.-Y. Wang, *Dalton Trans.*, 2014, **43**, 5823.
33 X. Zhou, P. Liu, W.-H. Huang, M. Kang, Y.-Y. Wang and Q.-Z. Shi, *CrystEngComm*, 2013, **15**, 8125.
34 D. Singh and C. M. Nagaraja, *Dalton Trans.*, 2014, **43**, 17912.
35 J.-M. Hao, B.-Y. Yu, K. V. Hecke and G.-H. Cui, *CrystEngComm*, 2015, **17**, 2279.
36 S. Sanda, S. Parshamoni, S. Biswas and S. Konar, *Chem. Commun.*, 2015, **51**, 6576.
37 Y. Wu, G.-P. Yang, X. Zhou, J. Li, Y. Ning and Y.-Y. Wang, *Dalton Trans.*, 2015, **44**, 10385.
38 L. E. Kreno, K. Leong, O. K. Farha, M. Allendorf, R. P. Van Duyne and J. T. Hupp, *Chem. Rev.*, 2012, **112**, 1105.
39 Z. Hu, B. J. Deibert and J. Li, *Chem. Soc. Rev.*, 2014, **43**, 5815–5840.
40 J.-W. Cui, W.-J. An, K. V. Hecke and G.-H. Cui, *Dalton Trans.*, 2016, **45**, 17474.
41 *APEX 2 software suite*, Bruker AXS Inc., Madison, Wisconsin, USA.
42 G. M. Sheldrick, SHELX, *Acta Crystallogr., Sect. A: Fundam. Crystallogr.*, 2008, **64**, 112.
43 C. B. Hübschle, G. M. Sheldrick and B. Dittrich, shelXle, *J. Appl. Crystallogr.*, 2011, **44**, 1281.
44 G.-X. Liu, K. Zhu, H. Chen, R.-Y. Huang, H. Xu and X.-M. Ren, *Inorg. Chim. Acta*, 2009, **362**, 1605.
45 Y. Gong, C. W. Hu, H. Li, K. L. Huang and W. Tang, *J. Solid State Chem.*, 2005, **178**, 3152.
46 A. Thirumurugan, M. B. Avinash and C. N. R. Rao, *Dalton Trans.*, 2006, 221.
47 S. Martínez-Vargas, A. Dorazco-González, S. Hernández-Ortega, R. A. Toscano, J. E. Barquera-Lozada and J. Valdés-Martínez, *CrystEngComm*, 2017, DOI: 10.1039/C7CE00871F, Advance Article; A. Dorazco-González, S. Martinez-Vargas, S. Hernández-Ortega and J. Valdés-Martínez, *CrystEngComm*, 2013, **15**, 5937; A. Dorazco-Gonzalez, R. A. Toscano, V. Gómez-Vidales and J. Valdés-Martínez, *Acta Crystallogr., Sect. E: Struct. Rep. Online*, 2006, **62**, m1027.
48 M. Yoon, H.-J. Sun, D.-H. Lee and G. Park, *Bull. Korean Chem. Soc.*, 2012, **33**, 3111.

49 X. Wang, W. Yao, Y.-F. Qi, M.-F. Luo, Y.-H. Wang, H.-W. Xie, Y. Yu, R.-Y. Maa and Y.-G. Li, *CrystEngComm*, 2011, **13**, 2542.

50 V. A. Blatov and D. M. Proserpio, *ToposPro 5.0*, 2015; V. A. Blatov, *IUCr CompComm. Newslett.*, 2006, **7**, 4; V. A. Blatov, *Struct. Chem.*, 2012, **23**, 955.

51 E. Cremades, J. Echeverria and S. Alvarez, *Chem. – Eur. J.*, 2010, **16**, 10380.

52 R. van Gorkum, F. Buda, H. Kooijman, A. L. Spek, E. Bouwman and J. Reedijk, *Eur. J. Inorg. Chem.*, 2005, 2255.

53 R. Alizadeh and V. Amani, *Inorg. Chim. Acta*, 2016, **443**, 151; I. Uçar, O. Z. Yeşilel, A. Bulut, H. Içbudak, H. Ölmez and C. Kazaka, *Acta Crystallogr., Sect. C: Cryst. Struct. Commun.*, 2004, **60**, 392.

54 Y. Gong, C. Hu, H. Li, K. L. Huang and W. Tang, *J. Solid State Chem.*, 2005, **178**, 3152.

55 R. Sen, D. Mal, P. Brandão, R. A. S. Ferreira and Z. Lin, *Cryst. Growth Des.*, 2013, **13**, 5272.

56 C. C. R. Sutton, G. da Silva and G. V. Franks, *Chem. – Eur. J.*, 2015, **21**, 6801.

57 J. Heine and K. Müller-Buschbaum, *Chem. Soc. Rev.*, 2013, **42**, 9232.

58 L.-Y. Zhang, J.-P. Zhang and Y.-Y. Lin, *Cryst. Growth Des.*, 2006, **6**, 1684.

59 X. Wang, C. Qin, E. Wang, Y. Li, N. Hao, C. Hu and L. Xu, *Inorg. Chem.*, 2004, **43**, 1850.

60 J. Tao, M.-L. Tong, J.-X. Shi, X.-M. Chen and S. W. Ng, *Chem. Commun.*, 2000, **20**, 2044.

61 K. Xing, R. Fan, S. Gao, X. Wang, X. Du, P. Wang, R. Fang and Y. Yang, *Dalton Trans.*, 2016, **45**, 4863.

62 L.-Y. Zhang, G.-F. Liu, S.-L. Zheng, B.-H. Ye, X.-M. Zhang and X.-M. Chen, *Eur. J. Inorg. Chem.*, 2003, 2965.

63 L. Zhang, Z. Kang, X. Xin and D. Sun, *CrystEngComm*, 2015, **18**, 193.

64 Y. Wu, G.-P. Yang, X. Zhou, J. Li, Y. Ning and Y.-Y. Wang, *Dalton Trans.*, 2015, **44**, 10385.

65 S. Dhanya and P. K. Bhattacharyya, *J. Photochem. Photobiol., A*, 1992, **63**, 179.

66 K. Müller-Buschbaum, F. Beuerle and C. Feldmann, *Microporous Mesoporous Mater.*, 2014, **216**, 171.

67 Y. Rachuri, B. Parmar, K. K. Bisht and E. Suresh, *Dalton Trans.*, 2017, **46**, 3623.

68 L. Zhai, W.-W. Zhang, J.-L. Zuo and X.-M. Ren, *Dalton Trans.*, 2016, **45**, 11935.

69 M. K. Salomón-Flores, I. J. Bazany-Rodríguez, D. Martínez-Otero, M. A. García-Eleno, J. J. Guerra-García, D. Morales-Morales and A. Dorazco-González, *Dalton Trans.*, 2017, **46**, 4950; A. Dorazco-Gonzalez, *Organometallics*, 2014, **33**, 868.

70 J. L. Du, X. Lu, T. L. Shen, C. P. Li, Y. J. Mu and L. J. Li, *Mater. Lett.*, 2015, **158**, 225.

71 J. M. Zhou, W. Shi, N. Xu and P. Cheng, *Inorg. Chem.*, 2013, **52**, 8082.

72 J.-H. Wang, M. Li and D. Li, *Chem. Sci.*, 2013, **4**, 1793.

73 X.-H. Jin, J.-K. Sun, L.-X. Cai and J. Zhang, *Chem. Commun.*, 2011, **47**, 2667.

74 A. L. Spek, *PLATON, A Multipurpose Crystallographic Tool*, Utrecht, the Netherlands, 1998; A. L. Spek, *J. Appl. Crystallogr.*, 2003, **36**, 7.

75 S. Halder, P. Ghosh, C. Rizzoli, P. Banerjee and P. Roy, *Polyhedron*, 2017, **123**, 217.

76 X. Zhang, W. Wang, Z. Hu, G. Wang and K. Uvdal, *Coord. Chem. Rev.*, 2015, **284**, 206.